nature biotechnology

Photoswitchable cyan fluorescent protein for protein tracking

Dmitriy M Chudakov[1,4], Vladislav V Verkhusha[2,4], Dmitry B Staroverov[3], Ekaterina A Souslova[1], Sergey Lukyanov[1] & Konstantin A Lukyanov[1]

In recent years diverse photolabeling techniques using green fluorescent protein (GFP)-like proteins have been reported[1–7], including photoactivatable PA-GFP[1], photoactivatable protein Kaede[2], the DsRed 'greening' technique[3] and kindling fluorescent proteins[6,7]. So far, only PA-GFP, which is monomeric and gives 100-fold fluorescence contrast, could be applied for protein tracking. Here we describe a dual-color monomeric protein, photoswitchable cyan fluorescent protein (PS-CFP). PS-CFP is capable of efficient photoconversion from cyan to green, changing both its excitation and emission spectra in response to 405-nm light irradiation. Complete photoactivation of PS-CFP results in a 1,500-fold increase in the green-to-cyan fluorescence ratio, making it the highest-contrast monomeric photoactivatable fluorescent protein described to date. We used PS-CFP as a photoswitchable tag to study trafficking of human dopamine transporter in living cells. At moderate excitation intensities, PS-CFP can be used as a pH-stable cyan label for protein tagging and fluorescence resonance energy transfer applications.

GFP and homologous fluorescent proteins are commonly used to visualize protein localization in living cells. In combination with photobleaching technique fluorescent proteins can also provide some information on the movement of intracellular proteins. However, photobleaching does not allow direct visualization of protein movement routes within a living cell. Recent studies resulted in the development of several photoactivatable fluorescent proteins[1–4,6,7]. Introduction of a photoactivatable fluorescent label makes possible precise photolabeling and tracking of the protein of interest and thus gives more complete information on its movement velocity and pathways. However, to provide for the protein tracking, a photoactivatable fluorescent protein must be monomeric, since an oligomeric fusion tag often results in improper protein functioning and aggregation.

In our search for monomeric photoactivatable GFP variants, we carried out site-directed mutagenesis of aceGFP (a fluorescent mutant of monomeric colorless *Aequorea coerulescens* protein[8]) at amino acid positions spatially close to the chromophore. In particular, saturation mutagenesis at positions 148 and 165 was conducted in combination with different variants at positions 220 and 222 (numbering coincides with *Aequorea victoria* GFP). The mutants Thr148-Phe165-Tyr220-Glu222 and Ser148-Leu165-Tyr220-Glu222 were cyan fluorescent and capable of photoconversion to a green fluorescent form in response to 405-nm light irradiation. We then used random mutagenesis of these two mutants to optimize their folding, brightness and contrast after photoactivation. The best photoactivatable variant selected, designated PS-CFP, contains substitutions T62A, N121S, H148T, K158R, I167V, E172K, F221L, G222E and K238Q, as compared to aceGFP. PS-CFP is also four amino acids longer, having a C-terminal extension WKLN (GenBank accession no. AY533824).

PS-CFP fluorescence excitation peaked at 402 nm, indicating the neutral chromophore absorption band[9]. In contrast to the customary fluorescence of the protonated chromophore in GFP, where excited-state proton transfer (ESPT) precedes green photon emission[10–12], PS-CFP emits photons in the cyan part of the visible spectrum (emission peaked at 468 nm), similar to the previously reported GFP-based ratiometric dual emission pH sensors[13,14]. ESPT is probably slowed down in PS-CFP because the chromophore environment modifies the proton-transfer networks. In particular, the combination of Thr148 and the spatially constraining Tyr220 and Glu222 may especially contribute to this effect.

In response to relatively intense 405-nm light irradiation (see below), PS-CFP underwent irreversible photoconversion, with a decrease in cyan fluorescence and appearance of a 490-nm excitation peak with an emission maximum at 511 nm. After complete photoconversion of PS-CFP took place, we observed a 300-fold green fluorescence increase and a fivefold cyan fluorescence decrease. This amounts to a 1,500-fold increase in the green-to-cyan fluorescence ratio, making PS-CFP the highest-contrast monomeric photoactivatable fluorescent protein. We demonstrated this effect in *Escherichia coli* colonies expressing PS-CFP (**Fig. 1**).

Phototransformation of a cyan fluorescent protein to a green fluorescent protein has not been observed before. However, we suggest that the explanation for this process is probably similar to that for *Aequorea victoria* GFP, where Glu222 is thought to be decarboxylated during photoconversion, leading to rearrangement of the hydrogen-bonding network, chromophore deprotonation and red shift of the

[1]Institute of Bioorganic Chemistry RAS, Laboratory of Genes for Regeneration, Miklukho-Maklaya 16/10, Moscow 117997, Russia. [2]Department of Pharmacology, University of Colorado Health Sciences Center, Denver, Colorado 80262, USA. [3]Evrogen JSC, Miklukho-Maklaya 16/10, Moscow 117997, Russia. [4]These authors contributed equally to this work. Correspondence should be addressed to K.A.L. (kluk@ibch.ru).

Published online 24 October 2004; doi:10.1038/nbt1025

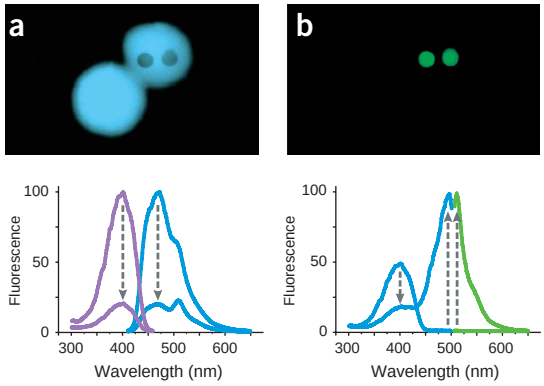

Figure 1 PS-CFP photoswitching. *E. coli* colonies expressing PS-CFP as seen through a fluorescent microscope. Two round areas of one colony were pre-irradiated by intense 405-nm light. Corresponding graphs show PS-CFP fluorescence spectra before and after complete photoactivation *in vitro*. Spectral changes in the course of photoactivation are shown with arrows. (**a**) *E. coli* colonies in the violet excitation light. Graphs show emission spectra in 402-nm excitation light (blue lines) and excitation spectra for 468-nm emission (violet lines). (**b**) The same colonies in the blue (460–490 nm) excitation light. Graphs show emission spectra in 490-nm excitation light (green lines) and excitation spectra for 511-nm emission (blue lines).

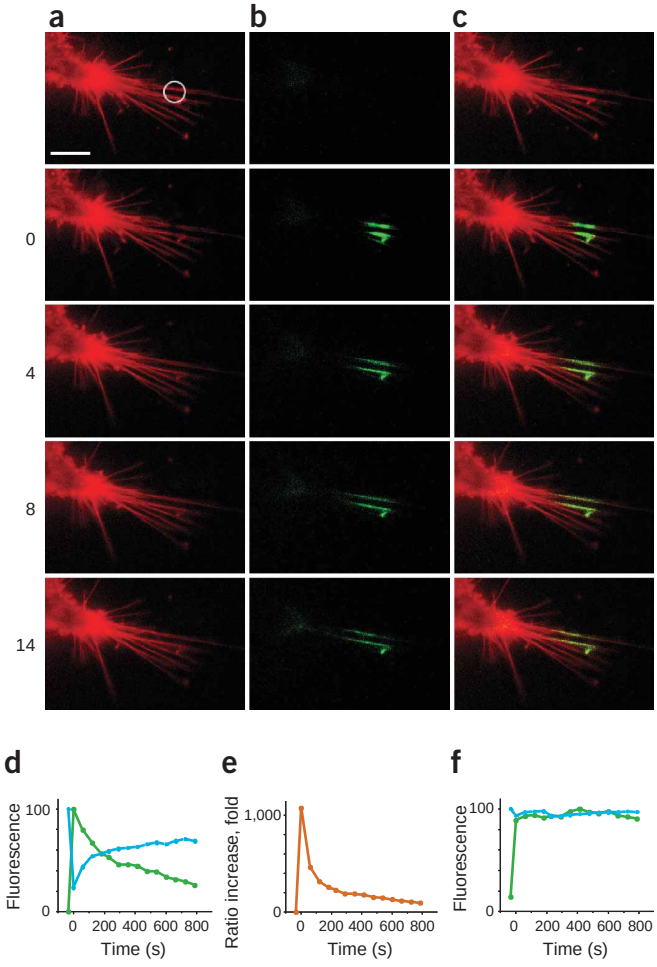

Figure 2 PS-CFP-hDAT tracking within filopodia of HEK293 cells. (**a**–**c**) Signals in ECFP (**a**) and FITC (**b**) channels are shown in red and green pseudocolors, respectively, and combined in the overlay (**c**). Circle indicates the photoswitched region. Scale bar, 10 μm. Time after photoactivation, in minutes, is shown on the left. (**d**–**f**) Normalized cyan (blue lines) and green (green lines) fluorescence changes and green-to-cyan fluorescence ratio growth, fold (red line) in the center of activated part of one filopodia (**d**,**e**) and within the whole shown region (**f**). Time zero corresponds to the first capture after activation.

excitation peak[15–17]. The same mechanism was proposed for PA-GFP photoactivation[1].

Before photoswitching, PS-CFP has a molar extinction coefficient of 34,000 $M^{-1}cm^{-1}$ and a fluorescence quantum yield of 0.16 (excitation/emission peaked at 402/468 nm). Photoswitched PS-CFP has a molar extinction coefficient of 27,000 $M^{-1}cm^{-1}$ and a fluorescence quantum yield of 0.19 (excitation/emission peaked at 490/511 nm), resulting in approximately the same brightness. The equal brightness of the cyan and green fluorescence signals may favor ratiometric measurement. Although photoactivated PS-CFP was about 2.5-fold dimmer than photoactivated PA-GFP, ratiometric measurement using PS-CFP gave better signal contrast (1,500-fold) than the intensity measurement using PA-GFP (100-fold). See **Supplementary Table 1** online for the comparison of PS-CFP with other photoactivatable GFP-like proteins.

PS-CFP displayed high pH stability, with a pK_a of 4.0 before photoactivation. No changes were observed in the shape or amplitude of the fluorescence spectra within a pH range of 4.8 to 9.0. This makes it possible to target PS-CFP to acidic organelles such as endosomes and lysosomes. By contrast, enhanced CFP (ECFP) loses half of its fluorescence at pH 4.7 (ref. 18). After photoswitching, PS-CFP has a pK_a of 6.0, similar to that of other GFP-like proteins with a phenolate anion chromophore, such as enhanced GFP (EGFP). **Supplementary Fig. 1** online compares the dependence of PS-CFP fluorescence on pH before and after photoactivation with that of EGFP. The photobleaching half-time of the photoactivated PS-CFP is about 1.5-fold shorter as compared to that of EGFP (see **Supplementary Fig. 2** online) and close to that of ECFP[18], which should be sufficient for most applications.

PS-CFP was generated from aceGFP[8], whose monomeric nature was confirmed by gel-filtration analysis and work with fusion proteins. Because PS-CFP has inherited the monomeric nature of aceGFP (see **Supplementary Fig. 3** online), it should be of wide use for protein labeling and tracking. To verify the applicability of PS-CFP as a fluorescent tag, we tested protein expression in mammalian cells. Transient PS-CFP expression in different cell lines showed an evenly distributed cyan signal without aggregation. Fluorescence was clearly detectable 36 h after transfection. No cell toxicity was observed. To test the utility of PS-CFP for protein labeling, we fused it with cytoplasmic β-actin. Transient expression of this fusion in L929 cells showed bright and correct actin labeling. Stress fibers, focal contacts and cell processes were clearly visible. Neither a negative influence on cell adhesion and vitality nor nonspecific aggregation were observed, confirming that PS-CFP was monomeric (**Supplementary Fig. 4** online).

Next we studied the photoswitching properties of PS-CFP in living cells. Before photoswitching, no detectable green fluorescence at the fluorescein isothiocyanate (FITC) excitation (Ex. 490BP10 nm, Em. 528BP19 nm) was seen in human epithelial kidney (HEK293) cells expressing PS-CFP. In contrast, a strong cyan signal was observed in the ECFP channel. Upon irradiation with a 175-W Xenon lamp through a standard DAPI filter (360–400 nm) for several minutes or with a 10–15 micro Joules (about 5–10 W/cm^2) violet dye laser (404 nm) for a few seconds, the fluorescence observed in the FITC channel increased more than 100-fold.

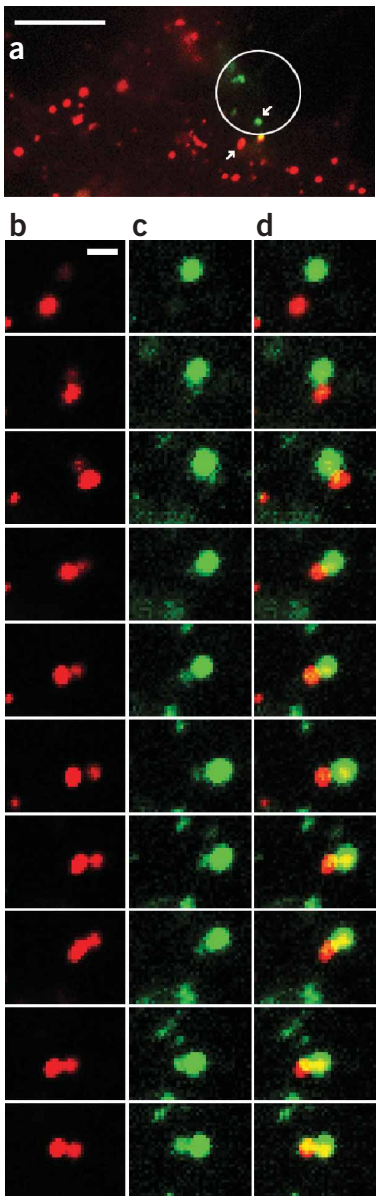

Figure 3 PS-CFP-hDAT interchange between two endosomes. Signals in ECFP and FITC channels are shown in red and green pseudocolors, respectively. (**a**) Cell region is shown 30 s after activation. Circle outlines the photoswitched region. Arrows point to endosomes tracked in **b**,**c**,**d**. Scale bar, 10 μm. (**b**–**d**) Two interacting endosomes exchange hDAT within a doublet. Scale bar, 1 μm. Time after the photoactivation, in minutes, is shown on the left. ECFP channel (**b**); FITC channel (**c**); overlay (**d**).

To test whether PS-CFP is suitable to study protein dynamics, we uniformly expressed PS-CFP throughout cells and selectively photoswitched a subpopulation of PS-CFP in the nucleus of one cell (see **Supplementary Fig. 5** online). Because of rapid diffusion within the nucleus, signals in the ECFP and FITC channels immediately equalized after photoswitching. Further imaging revealed a gradual decrease in the green signal and an increase in the cyan signal within the nucleus due to the movement of photoswitched PS-CFP through nuclear pores into the cytoplasm and of nonphotoswitched protein into the nucleus. This resulted in their equilibration through the cell within several minutes. Thus, photoswitching of PS-CFP can be used to mark a selected pool of intracellular molecules and then track dynamic changes in their localization.

We further applied PS-CFP to address a biological question about integral membrane protein trafficking. We focused on filopodia transport and constitutive endocytosis of a human dopamine transporter (hDAT), because both of them may control surface distribution of hDAT in the cell and thus represent a mechanism by which dopamine neurotransmission can be regulated. We fused PS-CFP to the N terminus of hDAT. A similar attachment of ECFP or enhanced yellow fluorescent protein (EYFP) did not affect hDAT functioning[19–21]. PS-CFP-hDAT was effectively transported along the biosynthetic pathway and localized in the membrane of HEK293 cells, including in multiple filopodia and microvilli (**Fig. 2a**, first panel). This was similar to the EYFP-hDAT expression pattern in cotransfection experiments (data not shown).

Applying 404-nm laser irradiation for a few seconds, we selectively photoswitched PS-CFP-hDAT in the middle parts of two thin filopodia. After photoactivation, a cyan fluorescence decrease of approximately fourfold and a green fluorescence increase of more than 250-fold were observed in the center of the activated filopodia region (**Fig. 2a–d**). Calculation of the green-to-cyan fluorescence ratio increased the primary contrast, resulting in a ratio change in this region of more than 1,000-fold (**Fig. 2e**). Movement of the photoswitched PS-CFP-hDAT started immediately and its speed reached 0.021–0.024 μm per second (**Fig. 2** and **Supplementary Videos 1** and **2** online). High PS-CFP contrast allowed us to monitor hDAT movement precisely within thin filopodia in the vicinity of a big PS-CFP-hDAT pool at the filopodia base. Moreover, after several minutes we could trace activated molecules entering this pool (**Fig. 2b**, last two panels). At the same time, a decrease in the cyan fluorescence during photoswitching allowed us to monitor nonswitched PS-CFP-hDAT molecules entering the activated region (**Fig. 2a**,**d**).

PS-CFP-hDAT translocation towards the cell cytoplasm was substantially greater than that towards filopodia tips, suggesting the involvement of some kind of hDAT retrograde-like transport. This differed from the all-directional diffusion observed for hDAT in the cell areas without ruffles and processes (data not shown).

Standard levels of excitation did not cause substantial photoswitching of cyan fluorescence or photobleaching of green fluorescence. For example, both cyan and green fluorescence of the whole region shown in **Figure 2** were rather stable in the course of an hDAT tracking experiment (**Fig. 2f**).

Heterologously expressed DAT has been shown to be endocytosed[19,21,22]. To test whether early endosomes can exchange cargo proteins such as hDAT, we selectively photoswitched PS-CFP-hDAT in several endosomes 0.7–0.9 μm in diameter (**Fig. 3a**). We tracked endosomes (both photolabeled and intact) within the whole cell for more than an hour after the photoactivation. Endosomes exhibited fast and rather chaotic intracellular movement, with a maximal speed of 0.16–0.18 μm per second. After 23 min, two endosomes drew together forming a doublet (**Fig. 3b–d** and **Supplementary Video 3** online). One of them contained photoswitched PS-CFP-hDAT, and soon after their contact we monitored a mutual exchange of PS-CFP-hDAT between the endosomes (**Fig. 3b–d**). Cyan fluorescence of the activated endosome recovered whereas green fluorescence of the second endosome grew. Direct exchange of cargo proteins between physically interacting endosomes has not been observed previously. At the same time, we did not observe substantial intensity changes in either the ECFP or FITC channel for noninteracting endosomes or for interacting nonphotoactivated endosomes. This indicates that in

contrast to endosomal protein components, including adaptor proteins[23], cargo proteins such as hDAT do not escape to the cytoplasm or enter endosomes during their sorting to different cellular compartments. Further studies are under way to reveal mechanisms of hDAT trafficking and endocytosis.

These experiments demonstrate the unique abilities of PS-CFP as a photoactivatable tag. First, PS-CFP is a high-contrast monomeric photoactivatable fluorescent protein. The ratio of green fluorescence of the activated and unactivated forms is three times higher for PS-CFP than for PA-GFP. Second, unlike PA-GFP, the PS-CFP emission spectrum changes completely during photoconversion, switching from cyan to green fluorescence. This allows calculation of the increase in the green-to-cyan fluorescence ratio and attainment of 1,500-fold increases. Third, the considerable cyan fluorescence decrease during photoconversion provides a molecular tool to track photoactivated protein movement simultaneously with its replacement with the nonactivated protein form (as shown in **Figs. 2** and **3**).

Earlier we described another contrasting photoactivatable protein, aceGFP-G222E[8]. However, photoactivation of this protein required a phototoxic 280-nm light irradiation and provided a very weak fluorescence both before and after the photoactivation, making it unsuitable as a photoactivatable tag.

One potential drawback of PS-CFP is that light of the same wavelength is used for photoconversion (high intensity) and initial cyan fluorescence visualization (standard intensity). In our experiments (see, for example, **Fig. 2f**) both cyan and green fluorescent signals were stable in the course of protein tracking experiments. However, in some applications undesirable PS-CFP switching during visualization can occur. Compared to PS-CFP, another ratiometric photoactivatable protein, Kaede[2], has the advantage of using light of different wavelengths for photoactivation and for visualizing the nonactivated form.

PS-CFP can still be used as a routine cyan fluorescent label at moderate excitation intensities (**Supplementary Fig. 4** online). The excitation spectrum of PS-CFP peaks at 402 nm, which is close to the excitation peak of enhanced blue fluorescent protein (EBFP). However, PS-CFP exhibits a large Stokes shift resulting in 468-nm peaked fluorescence close to ECFP emission. This allows the use of filters similar to those applied for ECFP emission and suggests that PS-CFP is a promising donor for fluorescence resonance energy transfer applications with yellow fluorescent acceptors. The high pH-stability of PS-CFP in acidic conditions (**Supplementary Fig. 1** online) and the unique positions of its excitation and emission peaks make it a worthy supplement to the existing palette of fluorescent proteins.

METHODS

Mutagenesis. Site-directed mutagenesis was done by overlap-extension PCR, with primers containing the appropriate target substitutions[24]. BD Clontech Diversity PCR Random Mutagenesis kit was used for random mutagenesis, in conditions optimal for seven mutations per 1,000 bp. *E. coli* colonies expressing mutant proteins were visually screened with a fluorescent stereomicroscope SZX-12 (Olympus). The best variants were selected and subjected to the next round of random mutagenesis.

Protein expression and spectral measurements. For bacterial expression, the full-length coding region was amplified using specific primers and inserted into the Qiagen pQE30 vector. Proteins fused to the N-terminal polyhistidine tag were expressed in *E. coli* XL1 Blue strain (Invitrogen) and purified using TALON metal-affinity resin (BD Clontech). Absorption spectra were recorded with Beckman DU520 UV/VIS Spectrophotometer. Varian Cary Eclipse fluorescence spectrophotometer was used for measuring excitation-emission spectra. For molar extinction coefficient determination, we relied on estimating mature chromophore concentration. Proteins were alkali-denatured with an equal volume of 2 M NaOH. Under these conditions, GFP chromophore absorbs at 446 nm and its molar extinction coefficient equals 44,000 $M^{-1}cm^{-1}$. Absorption spectra for native and alkali-denatured proteins were measured. On the basis of the absorption of denatured proteins, molar extinction coefficients for the native state were estimated. For quantum yield determination, the fluorescence of the mutants was compared with equally absorbing EGFP (quantum yield 0.60 (ref. 18)).

Expression in mammalian cell lines. For expression in eukaryotic cells, the PCR-amplified *Age*I-*Bgl*II fragment encoding PS-CFP was swapped with EGFP in the pEGFP-C1 vector (BD Clontech) resulting in pPS-CFP-C1 plasmid. To generate PS-CFP-β-actin fusion protein, PS-CFP was swapped with EGFP in the pEGFP-actin vector (BD Clontech). *Kpn*I-*Sma*I fragment encoding hDAT was cut out from the pEYFP-hDAT plasmid[21] and inserted into the respective sites of pPS-CFP-C1 resulting in pPS-CFP-hDAT plasmid. HEK293 and porcine aortic endothelial (PAE) cells were obtained from the American Type Culture Collection and cultured in Dulbecco's modified Eagle medium (DMEM; Invitrogen) and F-12 Nutrient Mixture (HAM; Invitrogen), respectively, supplemented with 10% FBS (Sigma) at 37 °C. Cells were transfected with pPS-CFP-C1 or pPS-CFP-hDAT plasmids using Effectene reagent (Qiagen). We replated cells 48 h after transfection on no. 1.0 round microscope cover glasses (Fisher Scientific) precoated with human fibronectin (Sigma). For hDAT internalization PAE cells were pretreated with 1 μM of phorbol ester (PMA) for 30 min at 37 °C. Live cell imaging was done 48 h later in DMEM or HAM without phenol red and containing 25 mM HEPES pH 7.5 (Invitrogen).

Microscopy and imaging. Fluorescence images of living cells were obtained using a digital microscope workstation based on Axiovert 200 M inverted microscope (Carl Zeiss) equipped with 175 W Xenon lamp source, 100× Plan-Apochromat 1.40 NA oil immersion objective lens, CoolSNAP HQ-cooled CCD camera (Roper Scientific), dual filter wheels, environmental chamber with thermocontroller (Carl Zeiss), and controlled by SlideBook 4.0 software (Intelligent Imaging Innovation). The workstation was equipped with Micropoint Ablation tunable dye laser system (Photonic Instruments) based on galvanometrically controlled scanning mirrors and nitrogen VSL-337ND-S pulse laser (Spectra-Physics). We routinely applied 404 nm dye, 10-Hz pulse rate and 15-micro Joules output laser power for PS-CFP photoswitching in living cells. Size and location of photoswithing area was adjusted with SlideBook 4.0 software. Total photoswitching time for living cells did not exceed 5-s 2 × 2 binning mode and 1-s exposure times were used for PS-CFP imaging through ECFP (Ex. 436BP10 nm, Em. 480BP20 nm) and FITC (Ex. 490BP10 nm, Em. 528BP19 nm) standard filters (Chroma). PS-CFP photoactivation in the *E. coli* colony was done using Nikon Optiphot fluorescent microscope, by 3-min irradiation through the violet filter (Ex. 405BP10, 100-W mercury lamp, 40× objective). Digital images were superimposed and assembled in Adobe Photoshop. Quantification of the image intensities was done with ImageJ software.

Note: Supplementary information is available on the Nature Biotechnology website.

ACKNOWLEDGMENTS

We are grateful to Alexander Sorkin for cDNA of hDAT and valuable discussions. We thank Natalia E. Yelina for the critical reading of the manuscript. This work was supported by grants from National Institutes of Health/National Institute on Drug Abuse A DA014204 and National Institutes of Health/National Institute of General Medical Sciences GM070358 (to V.V.V.), Russian Academy of Sciences for the program "Molecular and Cell Biology" and EC FP-6 Integrated Project LSHG-CT-2003-503259.

COMPETING INTERESTS STATEMENT

The authors declare that they have no competing financial interests.

Received 5 March; accepted 16 August 2004
Published online at http://www.nature.com/naturebiotechnology/

1. Patterson, G.H. & Lippincott-Schwartz, J. A photoactivatable GFP for selective photolabeling of proteins and cells. *Science* **13**, 1873–1877 (2002).
2. Ando, R., Hama, H., Yamamoto-Hino, M., Mizuno, H. & Miyawaki, A. An optical marker based on the UV-induced green-to-red photoconversion of a fluorescent protein. *Proc. Natl. Acad. Sci. USA* **99**, 12651–12656 (2002).

3. Marchant, J.S., Stutzmann, G.E., Leissring, M.A., LaFerla, F.M. & Parker, I. Multi-photon-evoked color change of DsRed as an optical highlighter for cellular and subcellular labeling. *Nat. Biotechnol.* **19**, 645–649 (2001).
4. Yokoe, H. & Meyer, T. Spatial dynamics of GFP-tagged proteins investigated by local fluorescence enhancement. *Nat. Biotechnol.* **14**, 1252–1256 (1996).
5. Dunn, G.A., Dobbie, I.M., Monypenny, J., Holt, M.R. & Zicha, D. Fluorescence localization after photobleaching (FLAP): a new method for studying protein dynamics in living cells. *J. Microsc.* **205**, 109–112 (2002).
6. Chudakov, D.M., Feofanov, A.V., Mudrik, N.N., Lukyanov, S. & Lukyanov, K.A. Chromophore environment provides clue to "kindling fluorescent protein" riddle. *J. Biol. Chem.* **278**, 7215–7219 (2003).
7. Chudakov, D.M. *et al.* Kindling fluorescent proteins for precise *in vivo* photolabeling. *Nat. Biotechnol.* **21**, 191–194 (2003).
8. Gurskaya, N.G. *et al.* A colourless GFP homologue from the non-fluorescent hydromedusa *Aequorea coerulescens* and its fluorescent mutants. *Biochem J.* **373**, 403–408 (2003).
9. Tsien, R.Y. The green fluorescent protein. *Annu. Rev. Biochem.* **67**, 509–544 (1998).
10. Chattoraj, M., King, B.A., Bublitz, G.U. & Boxer, S.G. Ultra-fast excited state dynamics in green fluorescent protein: multiple states and proton transfer. *Proc. Natl. Acad. Sci. USA* **93**, 8362–8367 (1996).
11. Creemers, T.M., Lock, A.J., Subramaniam, V., Jovin, T.M. & Volker, S. Three photoconvertible forms of green fluorescent protein identified by spectral hole-burning. *Nat. Struct. Biol.* **6**, 557–560 (1999).
12. Lill, M.A. & Helms, V. Proton shuttle in green fluorescent protein studied by dynamic simulations. *Proc. Natl. Acad. Sci. USA* **99**, 2778–2781 (2002).
13. Hanson, G.T. *et al.* Green fluorescent protein variants as ratiometric dual emission pH sensors. 1. Structural characterization and preliminary application. *Biochemistry* **41**, 15477–15488 (2002).
14. McAnaney, T.B., Park, E.S., Hanson, G.T., Remington, S.J. & Boxer, S.G. Green fluorescent protein variants as ratiometric dual emission pH sensors. 2. Excited-state dynamics. *Biochemistry* **41**, 15489–15494 (2002).
15. Brejc, K. *et al.* Structural basis for dual excitation and photoisomerization of the *Aequorea victoria* green fluorescent protein. *Proc. Natl. Acad. Sci. USA* **94**, 2306–2311 (1997).
16. Van Thor, J.J., Gensch, T., Hellingwerf, K.J. & Johnson, L.N. Phototransformation of green fluorescent protein with UV and visible light leads to decarboxylation of glutamate 222. *Nat. Struct. Biol.* **9**, 37–41 (2002).
17. Ehrig, T., O'Kane, D.J. & Prendergast, F.G. Green-fluorescent protein mutants with altered fluorescence excitation spectra. *FEBS Lett.* **367**, 163–166 (1995).
18. Patterson, G., Day, R.N. & Piston, D. Fluorescent protein spectra. *J. Cell Sci.* **114**, 837–838 (2001).
19. Daniels, G.M. & Amara, S.G. Regulated trafficking of the human dopamine transporter. Clathrin-mediated internalization and lysosomal degradation in response to phorbol esters. *J. Biol. Chem.* **274**, 35794–35801 (1999).
20. Carvelli, L. *et al.* PI 3-kinase regulation of dopamine uptake. *J. Neurochem.* **81**, 859–869 (2002).
21. Sorkina, T., Doolen, S., Galperin, E., Zahniser, N.R. & Sorkin, A. Oligomerization of dopamine transporters visualized in living cells by fluorescence resonance energy transfer microscopy. *J. Biol. Chem.* **278**, 28274–28283 (2003).
22. Saunders, C. *et al.* Amphetamine-induced loss of human dopamine transporter activity: an internalization-dependent and cocaine-sensitive mechanism. *Proc. Natl. Acad. Sci. USA* **97**, 6850–6855 (2000).
23. Sorkin, A. & Von Zastrow, M. Signal transduction and endocytosis: close encounters of many kinds. *Nat. Rev. Mol. Cell Biol.* **3**, 600–614 (2002).
24. Ho, S.N., Hunt, H.D., Horton, R.M., Pullen, J.K. & Pease, L.R. Site-directed mutagenesis by overlap extension using the polymerase chain reaction. *Gene* **77**, 51–59 (1989).